On Phase II SPC In Cases When Normality Is Invalid

Peihua Qiu and Jingnan Zhang
Department of Biostatistics
University of Florida

Abstract

Conventional statistical process control (SPC) charts require the normality assumption on the process response distribution. In reality, this assumption is often invalid. In such cases, it has been well demonstrated in the literature that results from control charts using the normality assumption may not be reliable in the sense that their actual false alarm rates could be substantially larger or smaller than the assumed false alarm rate. In this paper, we explore one natural solution to the phase II SPC problem in cases when the normality assumption is invalid, which tries to define a transformation based on an IC dataset so that the transformed process response distribution is close to normal and thus the conventional SPC charts can be applied to the transformed phase II data. This approach is compared with several alternative approaches in the literature, and some practical guidelines are provided regarding the use of all relevant control charts.

Keywords: Comparison; Data categorization; False alarm rate; Nonparametric SPC; Normality assumption; Robustness; Transformation; Wilcoxon rank-sum.

1 Introduction

Statistical process control (SPC) charts are widely used in industry for monitoring the stability of some sequential processes (e.g., manufacturing processes, health care systems, internet traffic flow, and so forth). Traditional control charts require the assumption that the process response distribution is normal. In practice, however, the normality assumption is often invalid. This paper discusses some strategies to construct control charts without the normality assumption.

As pointed out in Subsection 2.3.1 of Qiu[1], normal distributions play an important role in statistics, because many continuous numerical variables in practice roughly follow normal distributions and much statistical theory is developed for normally distributed random variables. An intuitive

explanation about the reason why many continuous numerical variables in our daily life roughly follow normal distributions can be given using the central limit theorem (CLT). For instance, a quality characteristic in question (e.g., the lifetime of a machine) is often affected by many different factors, including the quality of the raw material, labor, manufacturing facilities, proper operation in the manufacturing process, and so forth. So, by the CLT, its distribution would be roughly normal. By similar reasons, most existing SPC charts are developed based on the assumption that the related quality characteristics follow a normal distribution when the production process in question is in-control (IC) or after it becomes out-of-control (OC)[1–3]. It should be pointed out that a large dataset has nothing to do with the validity of the normality assumption on the quality characteristic variables. This is a common conceptual mistake made in the engineering literature.

In practice, however, there are many quality characteristic variables whose distributions are substantially different from normal distributions. For instance, economic indices and other non-negative indices are often skewed to the right. The lifetimes of products can often be described by Weibull distributions which could be substantially different from normal distributions. In many cases, it is difficult to find a parametric distribution to describe the distribution of certain quality characteristic variables. See real-data examples in papers by Qiu and Hawkins[4,5] and Qiu and Li[6]. In cases when the normality assumption is invalid, several authors[4, 7–10] have pointed out that the conventional control charts would be unreliable for process monitoring because their actual false alarm rates could be substantially larger or smaller than the assumed false alarm rate. In cases when the actual false alarm rate of a control chart is larger than the assumed false alarm rate, much labor and many other resources would be wasted because the production process is stopped too often in such cases. On the other hand, if the actual false alarm rate of a control chart is smaller than the assumed false alarm rate, then the chart cannot give signals of process distributional shift in a timely manner. A direct consequence could be that many defective products are manufactured without notice.

To handle cases when the normality assumption is invalid, a number of distribution-free or nonparametric control charts have been developed in the literature[4–6, 11–29]. Chakraborti et al.[30] and Qiu[1] gave a quite thorough overview on this topic. Most existing nonparametric control charts are based on the ranking information among observations at different time points[18,19,26]. Some of them are based on data categorization and on categorical data analysis[6, 22]. It should be pointed out that, in the literature, people do not always make a clear distinction between the terminologies

of "nonparametric control charts" and "distribution-free control charts." In many papers, both terminologies are used to refer to the control charts that can be applied to cases when the process distribution does not have a parametric form. Some "distribution-free control charts" may not be really distribution-free, in the sense that their design may still depend on the process distribution, although they do not require a parametric form of the process distribution.

In cases when the related production process has been adjusted properly so that it works stably and satisfactorily (i.e., the process is IC), we can always collect a set of observations from its manufactured products for designing a control chart to online monitor the process. These observations constitute an IC dataset, and the online process monitoring problem is often called phase II SPC (cf., Qiu[1], Section 1.3). To handle phase II SPC in cases when the normality is invalid, one natural idea is to first find a transformation from the IC dataset such that the distribution of the transformed process observations is close to normal, and then a conventional control chart is applied to the transformed process observations. In this paper, we explore this idea, and compare the performance of the related control charts with that of some existing nonparametric control charts. Our basic conclusion, based on a numerical study presented in Section 3, is that this transformation approach should be used with a care. In many cases when the normality assumption is invalid, a nonparametric chart, such as those described in the previous paragraph, might be more reliable and effective to use.

It should be pointed out that the transformation approach has been considered in the paper by Qiu and Li[21]. However, in that paper, we considered cases when batch data (i.e., the sample size is bigger than 1 at each observation time) were available at each time point during a phase II SPC, and we tried to transform the data at each time point separately to normal distributed data using a parametric transformation family. So, the transformations used at different time points could be all different and they are all determined by phase II observations. The problem discussed in the current paper is different in that we try to determine a single transformation from an IC dataset, and this transformation is then applied to all phase II observations. In the current setup, the phase II data could be either single-observation data (i.e., the sample size is 1 at each observation time) or batch data at individual observation times.

The rest part of the paper is organized as follows. In Section 2, certain statistical methods for finding data transformations to normality are described. Numerical comparison of the related control charts is presented in Section 3. A real-data example is discussed in Section 4 to demonstrate

Table 1: Johnson's transformation system

Label	Transformation	Parameter Conditions	X Condition
S_B	$\gamma + \eta \log\left(\frac{x-\epsilon}{\lambda+\epsilon-x}\right)$	$\eta, \lambda > 0, -\infty < \gamma < \infty$	$\epsilon < x < \epsilon + \lambda$
		$-\infty < \epsilon < \infty$	
S_L	$\gamma + \eta \log(x - \epsilon)$	$\eta > 0, -\infty < \gamma < \infty$	$x > \epsilon$
		$-\infty < \epsilon < \infty$	
S_U	$\gamma + \eta \sinh^{-1}\left(\frac{x-\epsilon}{\lambda}\right)$	Same as those of S_B	$-\infty < x < \infty$

the application of the proposed transformation-based control charts. Several remarks conclude the paper in Section 5.

2 Parametric Data Transformations to Normality

Assume that we have an IC dataset $x_1, x_2, \ldots, x_M$ collected from a production process in cases when it is IC, and that it has been verified by routine normality tests that the dataset does not have a normal distribution. For phase II SPC, we would like to find a parametric transformation from this dataset such that the distribution of the transformed data is close to normal. If that parametric transformation can be found, then we can apply the conventional phase II SPC charts to the transformed phase II observations. In this section, we describe two methods to find such parametric transformations which have been popularly used in the statistical literature, and then apply them to the SPC problem.

The first method is based on the three parametric distribution families originally proposed by Johnson[31]. These distribution families with labels S_B, S_L and S_U are listed in Table 1. The subscripts B, L and U refer to the distribution support as bounded, lower-bounded, and unbounded. For these three distribution families, the corresponding transformation functions have certain ability to transform them to the standard normal distribution. For a given distribution F, Slifker and Shapiro[32] developed a criterion to classify it to one of the three families using the quantile ratio (QR) defined as

$$QR = \frac{(\tau_4 - \tau_3)(\tau_2 - \tau_1)}{(\tau_3 - \tau_2)^2},$$

where τ_j is the q_jth quantile of the distribution F, for $j = 1, 2, 3, 4$, $q_1 = \Phi(-3z), q_2 = \Phi(-z), q_3 =$

$\Phi(z), q_4 = \Phi(3z)$, Φ is the cdf of the standard normal distribution, and z is a parameter to choose. Slifker and Shapiro's suggested decision rule is

- if $QR < 1$, then classify F into the S_B family,
- if $QR = 1$, then classify F into the S_L family, and
- if $QR > 1$, then classify F into the S_U family.

Based on the above decision rule, Chou et al.[33] proposed an algorithm to determine a parametric transformation which can transform the IC dataset to a dataset with the standard normal distribution, which is briefly described below.

Step 1 For a given z value, compute the estimated QR value by

$$\widehat{QR} = \frac{(\widehat{\tau}_4 - \widehat{\tau}_3)(\widehat{\tau}_2 - \widehat{\tau}_1)}{(\widehat{\tau}_3 - \widehat{\tau}_2)^2},$$

where $\widehat{\tau}_j$ is the q_jth sample quantile obtained from the IC dataset, for $j = 1, 2, 3, 4$.

Step 2 Use the above decision rule and the estimated QR value to choose the transformation family, and compute the maximum likelihood estimates of the distribution parameters as well.

Step 3 For the transformed data by the estimated transformation obtained in Step 2, compute the value of the Shapiro-Wilk test statistic W, which can be accomplished using almost all statistical software packages. In R, the command is `shapiro.test()`.

Step 4 For each z value in the set $S = \{z : z = 0.25, 0.26, \ldots, 1.25\}$, compute the W value using the above three steps, and the final estimated transformation is chosen to be the one with the largest W value.

As a remark, although the Shapiro-Wilk test statistic W is used in the above algorithm suggested by Chou et al.[33], other statistics for testing the normality assumption can be used as well and the overall result should not change much as long as the normality test used is reasonably good.

In the literature, another popular parametric transformation is based on the following Box-Cox transformation family[34]:

$$BC_\alpha(x) = \begin{cases} \frac{x^\alpha - 1}{\alpha}, & \text{if } \alpha \neq 0 \\ \log(x), & \text{otherwise,} \end{cases}$$

where α is a parameter chosen by maximizing the Shapiro-Wilk normality test statistic W. Since this transformation is only applicable for data with all positive observations, we can use its generalized form in cases when some observations in a dataset are negative, which is defined as

$$BC_{\alpha,\lambda}(x) = \begin{cases} \frac{(x+\lambda)^\alpha - 1}{\alpha}, & \text{if } \alpha \neq 0 \\ \log(x + \lambda), & \text{otherwise,} \end{cases}$$

where $\lambda > 0$ is a parameter chosen large enough such that $x + \lambda > 0$ for any x in the given dataset.

After a parametric transformation is obtained for a given IC dataset, then we can apply the transformation to all phase II observations and apply the conventional control charts to the transformed phase II observations. For instance, assume that $\widehat{g}_J(x)$ is the Johnson transformation obtained by the 4-step algorithm of Chou et al. described above from the IC dataset and the phase II observations are $y_1, y_2, \ldots$. Then, the two-sided CUSUM chart applied to the transformed phase II observations has the charting statistics

$$\begin{aligned} C_n^+ &= \max\left(0, C_{n-1}^+ + z_n - k\right), \text{ for } n \geq 1, \\ C_n^- &= \min\left(0, C_{n-1}^- + z_n + k\right), \end{aligned} \tag{1}$$

where $C_0^+ = C_0^- = 0$, $z_n = \widehat{g}_J(y_n)$ for each n, and $k > 0$ is an allowance constant. The chart gives a signal of mean shift when

$$C_n^+ > h \qquad \text{or} \qquad C_n^- < -h, \tag{2}$$

where $h > 0$ is a control limit. For some commonly used k and ARL_0 values, the corresponding h values can be found in Table 4.1 of Qiu[1]. They can also be computed easily using the R-package spc.

It should be pointed out that, although the CUSUM chart (1)–(2) is used here, other SPC charts, such as the Shewhart and EWMA charts, can also be applied to the transformed data $\{z_n, n \geq 1\}$. Shewhart charts are popular in practice mainly because of their simplicity. Due to the facts that they are good at detecting relatively large and transient shifts and such shifts are common in phase I SPC, they provide a reasonably good statistical tool for phase I SPC. As a

comparison, the CUSUM and EWMA charts are usually for phase II SPC, because these charts are often good in detecting relatively small and persistent shifts which are often our major concern in phase II SPC. Between the CUSUM and EWMA charts, their performance is generally similar. The EWMA charts are easier to understand and implement. On the other hand, CUSUM charts have certain theoretical optimality properties; the corresponding theory for the EWMA charts is still lacking. For these reasons, both CUSUM and EWMA charts are popularly used in practice. See Chapters 4 and 5 in Qiu[1] for more detailed discussions.

At the end of this section, we would like to point out that although nonparametric methods for estimating distribution functions, such as the empirical distribution estimation method and the kernel density estimation method discussed in Section 2.8 of Qiu[1], can also be considered here, they are generally infeasible for phase II SPC for the two reasons explained below. First, assume that $\widehat{F}$ is an estimator of the cdf F of the IC process distribution. Then, the transformation $\Phi^{-1}[\widehat{F}(x)]$ can generally transform a random variable X with the cdf F to the random variable $\Phi^{-1}[\widehat{F}(X)]$ whose distribution is close to $N(0,1)$. If $\widehat{F}$ is a nonparametric estimator of F, then for every phase II observation y_n, we need to compute the value of $\widehat{F}(y_n)$ from the IC dataset, which takes much time because $\widehat{F}(y_n)$ does not have a parametric form and its value needs to be computed from all IC observations for every y_n. As a comparison, if $\widehat{F}$ is a parametric estimator, then the parametric function $\widehat{F}(x)$ is well estimated before the phase II process monitoring. In such cases, we only need to evaluate this function once for each phase II observation y_n. So, the computation involved in this case is much simpler. Second, if $\widehat{F}$ is a nonparametric estimator of F, then its variability is usually large. Consequently, phase II SPC based on $\widehat{F}$ is not effective, especially when the IC sample size M is relatively small. We actually tried the nonparametric method using the empirical estimator of F, and the results were not good in most cases considered. For these reasons, this approach is not considered in this paper.

3 Numerical Study

In this section, we evaluate the numerical performance of the CUSUM chart (1)-(2) based on the parametric transformations described in Section 2. The two versions of the CUSUM chart (1)-(2) based on the Johnson's transformation families and the Box-Cox transformation family are denoted as CUSUM-J and CUSUM-B, respectively. Besides these two transformation-based control charts,

the conventional CUSUM chart (i.e., the CUSUM chart (1)-(2) applied to the original phase II observations), denoted as CUSUM-C, and the two nonparametric CUSUM charts proposed by Li et al.[19] and Qiu and Li[6], denoted as CUSUM-L and CUSUM-Q, respectively, are also considered here for comparison purposes. The chart CUSUM-L is based on the Wilcoxon rank-sum test statistic for comparing the means of the IC observations and a phase II observation. The chart CUSUM-Q is based on categorization of phase II observations. The cut-points for observation categorization is estimated from the IC dataset. By the suggestion of Qiu and Li[6], the number of categories is chosen to be 5 in all numerical examples in this paper. For all five charts, the IC dataset is used for estimating the IC mean and IC standard deviation, and the phase II observations are standardized by the estimated IC mean and IC standard deviation. So, all five control charts depend on the IC dataset.

We first investigate the IC performance of the five CUSUM charts. In the charts CUSUM-C, CUSUM-J, CUSUM-B, and CUSUM-L, the allowance constant k is chosen to be 0.5. In the chart CUSUM-Q, the allowance constant is chosen to be 0.01 as suggested by Qiu and Li[6]. In all five charts, the assumed ARL_0 value is chosen to be 500. The control limits of the charts CUSUM-C, CUSUM-J, and CUSUM-B are all chosen to be $h = 5.072$ which is obtained by the R-package spc for the conventional CUSUM chart (1)-(2) in cases when the true process distribution is $N(0, 1)$. The control limits of the charts CUSUM-L and CUSUM-Q are obtained by simulation as follows. First, we generate an IC dataset of size M from the $N(0, 1)$ distribution. Then, the ARL_0 value of the chart under consideration with a control limit h_1 is computed based on 10,000 replicated simulations of phase II process monitoring. This entire process, from generating the IC dataset to computing the ARL_0 value, is then repeated 100 times, and the average of the 100 ARL_0 values and the corresponding standard error of this overall ARL_0 estimate can be computed. The h_1 value is then searched until the assumed ARL_0 value (i.e., 500) is reached within a certain accuracy. See the pseudo code given in Subsection 4.2.2 of Qiu[1] for a related discussion. In this example, we consider cases when the true process distribution is one of the following four distributions: $N(0, 1)$, t_4, χ^2_4 and χ^2_1, and the IC sample size $M = 50, 100$, 200, 500, or 1,000. The computed actual ARL_0 values of the five charts and their standard errors in all cases considered are presented in Table 2. From the table, it can be seen as expected that the conventional CUSUM chart CUSUM-C performs poorly in all non-normal cases considered. The chart CUSUM-J is reasonably reliable to handle symmetric distributions when $M \geq 500$. But, it performs poorly when handling skewed distributions, unless

M is very large. As a comparison, the chart CUSUM-B performs well when handling skewed distributions and when $M \geq 200$. But, it performs poorly to handle symmetric distributions, especially when the distribution has heavy tails. Its performance is not satisfactory even in the $N(0,1)$ case because it uses the estimated IC mean and IC standard deviation obtained from the IC dataset for standardising the phase II observations and the randomness in these estimators has a quite big impact on its performance, which is consistent with the findings in Jones et al.[35] Both the CUSUM-L and CUSUM-Q charts are quite reliable. Between the two charts, it seems that CUSUM-L has a more reliable performance.

Next, we study the OC performance of the five CUSUM charts in cases when $M = 500$, the true process distribution is one of the four distributions: $N(0,1)$, t_4, χ^2_4, and χ^2_1, and the process mean has a shift of size -1.0, -0.8, -0.6, -0.4, -0.2, 0, 0.2, 0.4, 0.6, 0.8, or 1.0. In all five CUSUM charts, their allowance constants are chosen to be the same as those in Table 2, but their control limits have been adjusted such that their actual ARL_0 values are all equal to 500 in order to make the comparison meaningful. For each shift size, the ARL_1 values of the five charts are computed in the same way as that for computing the ARL_0 values based on 1,000,000 replicated simulations. They are shown in the four plots of Figure 1. From Figure 1(a), it can be seen that the chart CUSUM-Q is the most effective one in cases with the $N(0,1)$ IC distribution, and the other four charts perform similarly in such cases. Readers are reminded again that the conventional chart CUSUM-C depends on the estimated IC mean and the estimated IC standard deviation obtained from the IC dataset and thus its performance is not the best in these cases. From Figure 1(b), the chart CUSUM-Q still performs the best in cases with the t_4 IC distribution, the charts CUSUM-J, CUSUM-B, and CUSUM-L perform similarly well, and the chart CUSUM-C performs the worst. From Figure 1(c)-(d), in which the process IC distribution is skewed, the chart CUSUM-Q still performs reasonably well, the charts CUSUM-J and CUSUM-L perform well in detecting shifts in the direction of the shorter tail of the process distribution and do not perform well in detecting shifts in the other direction, and the charts CUSUM-C and CUSUM-B do not perform well in these cases.

From the above examples, we can have the following conclusions. First, in cases when the process distribution is non-normal, the IC performance of the nonparametric CUSUM charts CUSUM-L, and CUSUM-Q is much better than the transformation-based CUSUM charts CUSUM-J and CUSUM-B, especially in cases when the IC sample size M is quite small. Second, when M is mod-

Table 2: Actual ARL_0 values and their standard errors (in parentheses) of the five charts CUSUM-C, CUSUM-J, CUSUM-B, CUSUM-L, and CUSUM-Q in cases when the true process distribution is one of the four distributions: $N(0,1)$, t_4, χ^2_4 and χ^2_1, and the IC sample size $M = 50, 100$, 200, 500, or 1,000.

	M	$N(0,1)$	t_4	χ^2_4	χ^2_1
CUSUM-C	50	382.888 (250.525)	250.200 (205.969)	283.673 (236.838)	172.408 (165.861)
	100	419.637 (207.654)	254.497 (164.393)	281.570 (192.550)	175.891 (123.687)
	200	445.403 (152.254)	273.403 (138.348)	271.690 (135.320)	161.215 (98.398)
	500	441.926 (100.754)	270.199 (90.543)	252.476 (86.057)	153.205 (45.654)
	1000	461.632 (75.302)	280.434 (91.822)	249.044 (63.204)	151.081 (30.268)
CUSUM-J	50	369.620 (242.069)	245.861 (208.249)	190.468 (180.156)	210.960 (194.732)
	100	419.981 (214.258)	370.054 (189.475)	301.840 (195.946)	255.321 (189.925)
	200	439.772 (153.220)	426.193 (176.501)	347.987 (170.446)	287.343 (172.375)
	500	436.556 (103.337)	448.818 (113.095)	409.316 (122.638)	367.177 (209.645)
	1000	461.023 (79.379)	504.009 (91.748)	453.970 (105.538)	419.313 (264.276)
CUSUM-B	50	328.129 (230.997)	150.827 (128.142)	345.846 (240.819)	426.078 (216.423)
	100	387.500 (206.079)	192.144 (136.465)	418.378 (177.347)	427.525 (203.283)
	200	425.248 (150.238)	204.951 (94.686)	452.338 (133.049)	457.110 (147.270)
	500	434.499 (100.228)	233.302 (76.723)	466.154 (88.147)	488.681 (86.533)
	1000	458.152 (76.042)	238.587 (48.855)	485.871 (71.402)	501.757 (62.586)
CUSUM-L	50	499.987 (475.261)	409.224 (297.308)	443.384 (381.543)	472.958 (387.439)
	100	500.409 (283.277)	480.287 (304.409)	478.479 (233.217)	506.940 (295.109)
	200	500.223 (184.396)	497.329 (187.008)	485.958 (132.297)	490.173 (177.090)
	500	500.855 (108.500)	516.224 (104.384)	504.302 (99.425)	514.469 (92.996)
	1000	500.506 (78.758)	504.290 (74.383)	494.360 (73.924)	500.741 (63.737)
CUSUM-Q	50	499.185 (1474.81)	493.056 (1459.65)	511.651 (1637.72)	528.151 (909.546)
	100	499.166 (665.627)	382.636 (350.420)	537.856 (766.362)	583.596 (914.399)
	200	499.602 (440.295)	468.637 (415.753)	431.746 (327.797)	506.741 (469.711)
	500	499.967 (231.967)	525.523 (249.106)	542.097 (259.191)	531.758 (244.535)
	1000	499.361 (153.236)	496.961 (145.510)	494.523 (147.364)	530.653 (150.743)

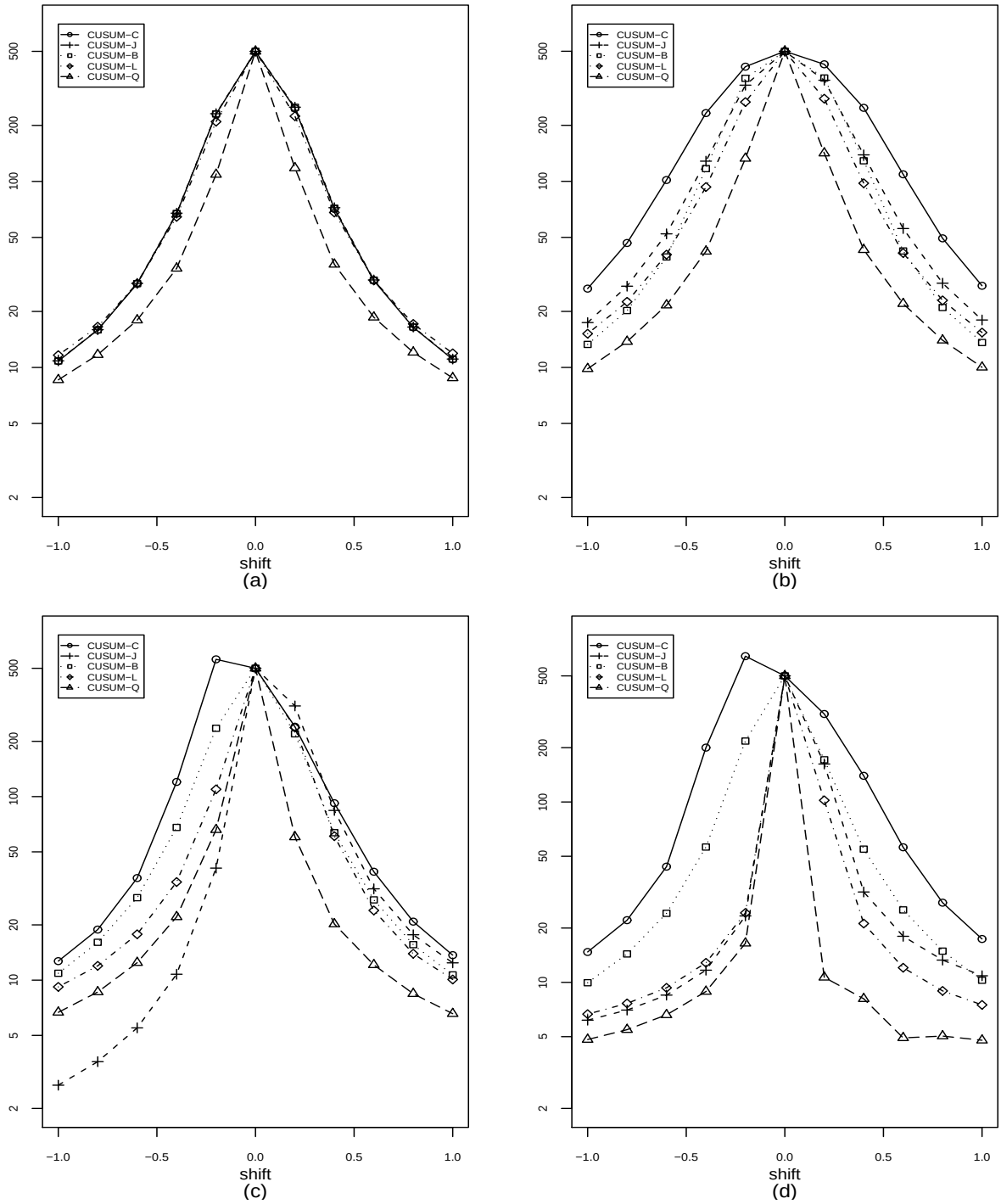

Figure 1: ARL_1 values of the charts CUSUM-C, CUSUM-J, CUSUM-B, CUSUM-L, and CUSUM-Q in cases when $M = 500$, $ARL_0 = 500$, and the true process distribution is $N(0, 1)$ (plot (a)), t_4 (plot (b)), χ^2_4 (plot (c)), or χ^2_1 (plot (d)).

erate to large and the process distribution is symmetric, the IC performance of CUSUM-J is quite reliable. As a comparison, when M is moderate to large and the process distribution is skewed, the IC performance of CUSUM-B is quite reliable. Third, results by the conventional CUSUM chart CUSUM-C is unreliable in cases when the process distribution is non-normal. Fourth, among all the five CUSUM charts considered, the chart CUSUM-Q is quite effective in detecting process mean shifts in almost all cases considered. As a comparison, the other four charts are quite effective only in certain special cases.

4 A Real-Data Application

In this section, we illustrate the application of the transformation-based CUSUM charts CUSUM-J and CUSUM-B using a real-data example about daily exchange rates between Korean Won and US Dollar between March 28, 1997 and December 02, 1997. During this period, the daily exchange rates were quite stable early on and became unstable starting from early August, due to the world financial crisis. This can be seen from Figure 2(a) in which 123 daily exchange rates (Won/Dollar) observed in that period are shown. Like many other phase II SPC procedures, charts CUSUM-J and CUSUM-B assume that observations at different time points are independent of each other. However, for this data, we found that observations are substantially correlated. Following the suggestions by Qiu and Hawkins[4], we first pre-whiten the data using an auto-regression model that can be accomplished by the R function ar.yw(), and the pre-whitened data are shown in Figure 2(b).

We then apply the related control charts considered in the previous section to the pre-whitened data. To this end, the first 107 residuals are used as an IC data and the remaining residuals are used for testing. In Figure 2(b), the training and testing data are separated by a dashed vertical line. To take a closer look at the IC data and at the first several testing observations as well, the first 144 residuals are presented in Figure 2(c) again, in which the solid horizontal line denotes the sample mean of the IC data and the dashed vertical line separates the IC data and testing data. From Figure 2(c), it can be seen that there is an upward mean shift starting from the very beginning of the test data. The Shapiro test for checking the normality of the IC data gives a p-value of 7.807×10^{-5}, implying that the IC data are significantly non-normal. To demonstrate this, the density histogram of the IC data is shown in Figure 2(d), along with its estimated density curve

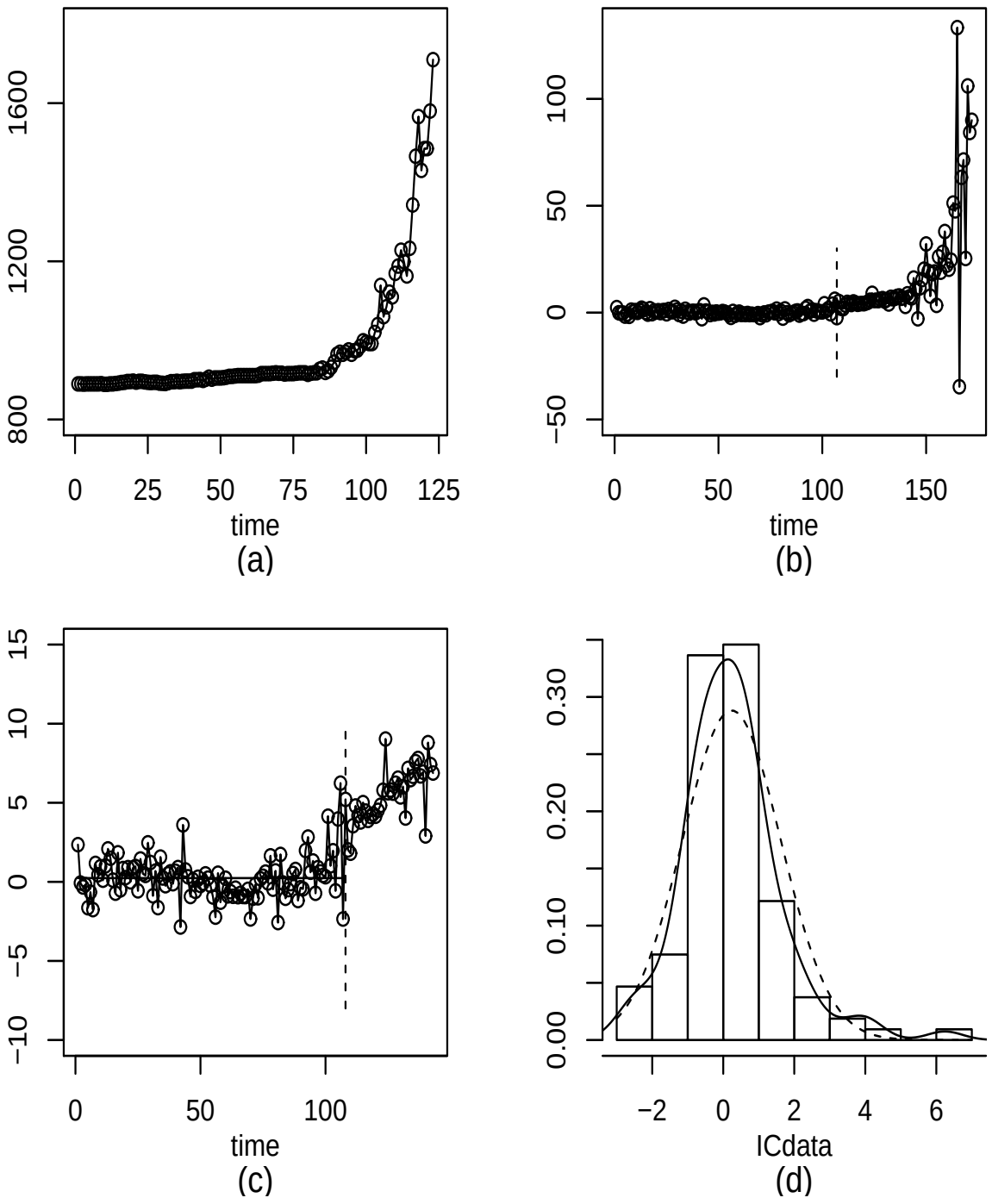

Figure 2: (a) Original observations of the exchange data. (b) Pre-whitened data. (c) The first 144 pre-whitened values. (d) Density histogram, estimated density curve (solid) of the first 107 pre-whitened values (i.e., IC data), and the density curve of a normal distribution (dashed) with the same mean and variance as those of the IC data. In plots (b)–(c), the dashed vertical lines separate the IC and testing data. In plot (c), the solid horizontal line denotes the sample mean of the IC data.

(solid) and the density curve of a normal distribution (dashed) with the same mean and standard deviation. We then apply the related control charts to this dataset. The allowance constants of these charts are chosen to be the same as those used in the previous section, and their control limits are searched such that $ARL_0 = 500$. In the chart CUSUM-Q, the number of categories is still chosen to be 5. The five control charts are shown in Figure 3, in which the dashed horizontal lines denote the control limits of the related control charts. The charts CUSUM-C, CUSUM-J, CUSUM-B, CUSUM-L, and CUSUM-Q give signals of process mean shift at the 112th, 112th, 112th, 113th, and 111th time points, respectively. Therefore, the five charts perform similarly in this example. These control charts confirm that the exchange rates between Korean Won and US Dollar started to become unstable at the very beginning of the phase II monitoring, as demonstrated in Figure 2(c).

5 Concluding Remarks

This paper considers cases when the process distribution is non-normal. In such cases, if an IC dataset is available, a natural idea for phase II SPC is to find a parametric transformation based on the IC dataset such that the transformed process distribution is close to normal. Then, the conventional SPC charts can be applied to the transformed phase II observations for online process monitoring. In the previous sections, we have explored such an idea by using the two popular parametric distributions (i.e., the Johnson's transformation system and the Box-Cox transformation family) and by comparing the CUSUM charts obtained by this idea with two representative nonparametric CUSUM charts. Based on the numerical results presented in the previous two sections, we can conclude that the nonparametric CUSUM charts are generally more reliable to use in cases when the process distribution is non-normal in the sense that their actual ARL_0 values are usually closer to the assumed ARL_0 value than the ARL_0 values of the transformation-based CUSUM charts. The performance of the transformation-based CUSUM charts could be potentially improved by combining the IC data with the observations collected during phase II SPC through a self-starting framework, which needs to be confirmed in our future research. Furthermore, the nonparametric CUSUM chart CUSUM-Q seems much more effective in detecting process mean shifts in various non-normal cases considered, compared to the transformation-based CUSUM charts. In multivariate SPC, we might have similar conclusions, which needs to be confirmed in the future research as well.

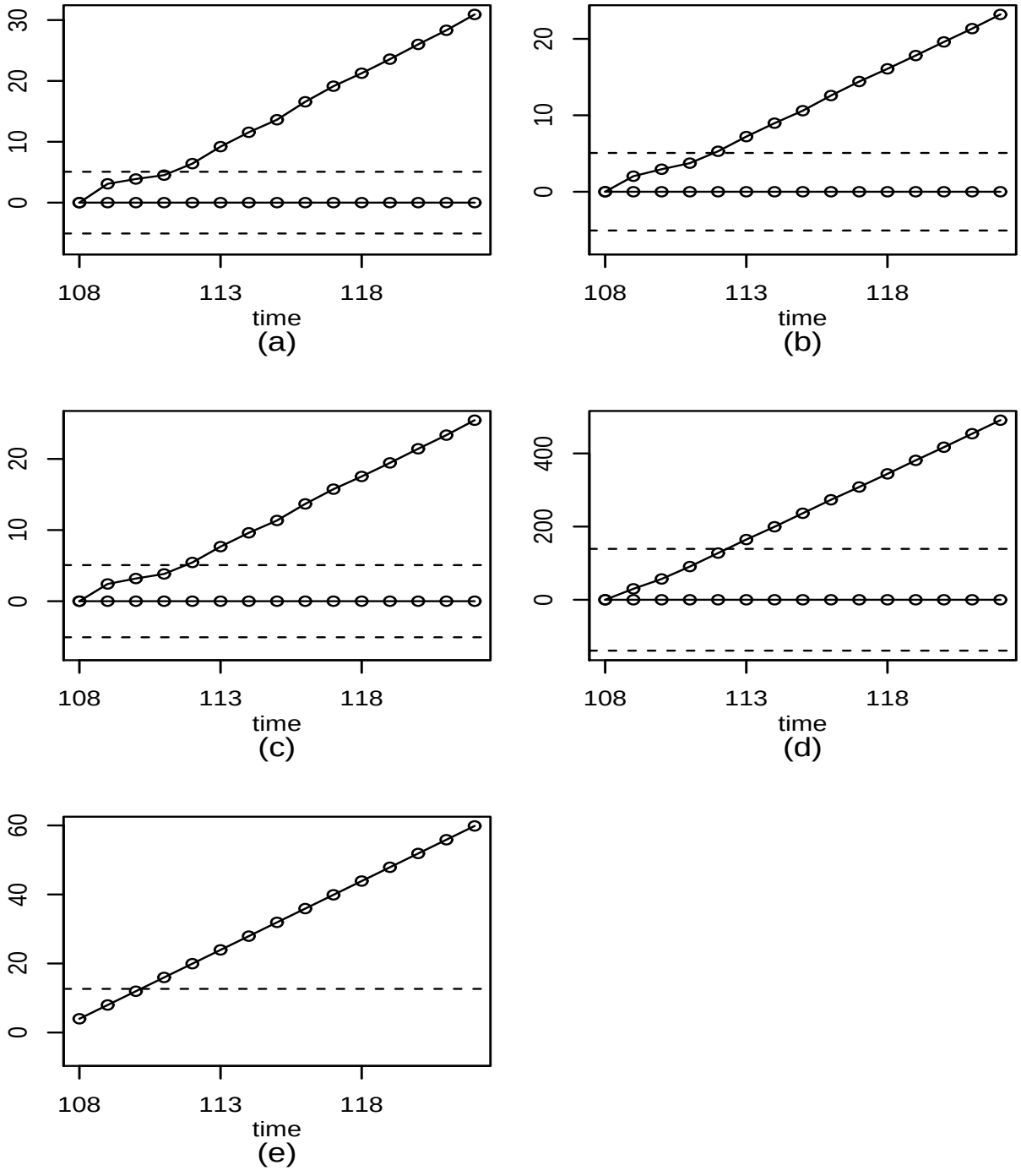

Figure 3: Control charts CUSUM-C, CUSUM-J, CUSUM-B, CUSUM-L, and CUSUM-Q when they are applied to the exchange rate data. In each plot, the horizontal dashed line(s) denotes the control limit(s).

Acknowledgments

The authors thank one guest co-editor and two referees for their valuable comments which greatly improved the quality of this paper. This research is supported in part by an NSF grant.

References

1. Qiu P. *Introduction to Statistical Process Control*. Chapman & Hall/CRC: Boca Raton, FL, 2014.

2. Hawkins DM, Olwell DH. *Cumulative Sum Charts and Charting for Quality Improvement*. Springer-Verlag:New York,1998.

3. Montgomery DC. *Introduction To Statistical Quality Control (6th edn)*. John Wiley & Sons:New York, 2009.

4. Qiu P, Hawkins DM. A rank based multivariate CUSUM procedure. *Technometrics* 2001; **43**(2):120–132.

5. Qiu P, Hawkins DM. A nonparametric multivariate cumulative sum procedure for detecting shifts in all directions. *Journal of Royal Statistical Society:Series D (The Statistician)* 2003; **52**(2):151–164.

6. Qiu P, Li Z. On nonparametric statistical process control of univariate processes. *Technometrics* 2011a; **53**(4):390–405.

7. Amin R, Reynolds MR, Bakir ST. Nonparametric quality control charts based on the sign statistic. *Communications in Statistics-Theory and Methods* 1995; **24**(6):1597–1623.

8. Hackl P, Ledolter J. A new nonparametric quality control technique. *Communications in Statistics-Simulation and Computation* 1992; **21**:423–443.

9. Lucas JM, Crosier RB. Robust CUSUM: a robust study for CUSUM quality control schemes. *Communications in Statistics-Theory and Methods* 1982; **11**(23): 2669–2687.

10. Rocke DM. Robust control charts. *Technometrics* 1989; **31**(2):173–184.

11. Albers W, Kallenberg WCM. CUMIN charts. *Metrika* 2009; **70**(1):111–130.

12. Amin RW, Widmaier O. Sign control charts with variable sampling intervals. *Communications in Statistics: Theory and Methods* 1999; **28**(8):1961–1985.

13. Bakir ST. Distribution-free quality control charts based on signed-rank-like statistics. *Communications in Statistics-Theory and Methods* 2006; **35**:743–757.

14. Bakir ST, Reynolds MR. A nonparametric procedure for process control based on within group ranking. *Technometrics* 1979; **21**(2):175–183.

15. Chatterjee S, Qiu P. Distribution-free cumulative sum control charts using bootstrap-based control limits. *Annals of Applied Statistics* 2009; **3**(1):349–369.

16. Chakraborti S, Eryilmaz S, Human SW. A phase II nonparametric control chart based on precedence statistics with runs-type signaling rules. *Computational Statistics and Data Analysis* 2009; **53**(4):1054–1065.

17. Hackl P, Ledolter J. A control chart based on ranks. *Journal of Quality Technology* 1991; **23**:117–124.

18. Hawkins DM, Deng Q. A nonparametric change-point control chart. *Journal of Quality Technology* 2010; **42**:165–173.

19. Li SY, Tang LC, Ng SH. Nonparametric CUSUM and EWMA control charts for detecting mean shifts. *Journal of Quality Technology* 2010; **42**(2):209–226.

20. McDonald D. A CUSUM procedure based on sequential ranks. *Naval Research Logistics* 1990; **37**(5):627–646.

21. Qiu P, Li Z. Distribution-free monitoring of univariate processes. *Statistics and Probability Letters* 2011b; **81**(12):1833–1840.

22. Qiu P. Distribution-free multivariate process control based on log-linear modeling. *IIE Transactions* 2008; **40**:664–677.

23. Ross GJ, Tasoulis DK, Adams NM. Nonparametric monitoring of data streams for changes in location and scale. *Technometrics* 2011;**53**(4):379–389.

24. Willemain TR, Runger GC. Designing control charts using an empirical reference distribution. *Journal of Quality Technology* 1996; **28**(1):31–38.

25. Yashchin E. Analysis of CUSUM and other Markov-type control schemes by using empirical distributions. *Technometrics* 1992; **34**(1):54–63.

26. Zou C, Tsung F. Likelihood ratio-based distribution-free EWMA control charts. *Journal of Quality Technology* 2010; **42**(2):174–196.

27. Zhou C, Zou C, Zhang Y, Wang Z. Nonparametric control chart based on change-point model. *Statistical Papers* 2009; **50**:13–28.

28. Zou C, Tsung F. A multivariate sign EWMA control chart. *Technometrics* 2011; **53**:84–97.

29. Zou C, Wang Z, Tsung F. A spatial rank-based multivariate EWMA control chart. *Naval Research Logistic* 2012; **59**:91–110.

30. Chakraborti S, van der Laan P, Bakir ST. Nonparametric control charts: an overview and some results. *Journal of Quality Technology* 2001; **33**(3):304–315.

31. Johnson NL. Systems of frequency curves generated by methods of translation. *Biometrika* 1949; **36**: 149–176.

32. Slifker JF, Shapiro SS. The johnson system: selection and parameter estimation. *Technometrics* 1980; **22**: 239–246.

33. Chou Y, Polansky AM, Mason RL. Transforming non-Normal Data to Normality in Statistical Process Control. *Journal of Quality Technology* 1998; **30**(2):133-141.

34. Box GEP, Cox DR. An Analysis of Transformations. *Journal of the Royal Statistical Society Series B (Methodological)* 1964; **26**(2): 211–252.

35. Jones LA, Champ CW, Rigdon SE. The run length distribution of the CUSUM with estimated parameters. *Journal of Quality Technology* 2004; **36**(1):95–108.